Dendrochronologia 97 (2026) 126537

Contents lists available at ScienceDirect

Dendrochronologia

journal homepage: www.elsevier.com/locate/dendro

Impact of canopy disturbances on climate sensitivity of old-growth beech (*Fagus sylvatica* L.) forests

Antonia Kölzer [a], Davide Frigo [b], Edurne Martinez del Castillo [a], Frederick Reinig [a], Jan Esper [a,c], Ingo Heinrich [d,e,f], Burkhard Neuwirth [g], Michele Baliva [h], Gianluca Piovesan [h], Emanuele Ziaco [a,*]

[a] Department of Geography, Johannes Gutenberg University, Mainz, Germany
[b] Department of Land, Environment, Agriculture and Forestry, University of Padova, Legnaro, Italy
[c] Global Change Research Institute (CzechGlobe), Czech Academy of Sciences, Brno, Czech Republic
[d] Department of Natural Sciences, German Archeological Institute (DAI), Berlin, Germany
[e] Section for Climate Dynamics and Landscape Evolution, German Research Centre for Geosciences, (GFZ), Potsdam, Germany
[f] Department of Geography, Humboldt-University Berlin, Germany
[g] DeLaWi Tree-Ring Analyses, Windeck, Germany
[h] DEB, Department of Ecological and Biological Sciences, University of Tuscia, Viterbo, Italy

ARTICLE INFO

Keywords:
Disturbance ecology
Radial growth releases
Climatic signal
Dendroclimatology
Boundary line release criteria
Gap dynamics

ABSTRACT

Canopy disturbances can affect tree growth and mask climate signals in tree rings. Their magnitude and lasting effects, however, remain poorly understood, potentially obscuring dendroclimatic analyses in closed-canopy forests. Here, we evaluate the influence of canopy disturbances on the climate sensitivity in European beech (*Fagus sylvatica* L.) in three old-growth forests spanning a wide range of ecoclimatic conditions. Growth-release detection was used to identify disturbed and undisturbed trees and assess their sensitivity to maximum temperature, precipitation, vapor-pressure deficit, diurnal temperature range, and cloud cover over two periods (1902–2022, 1962–2022). Our results indicate that, across all sites, growth was primarily driven by moisture availability and previous-season maximum temperature. While growth releases cause short-term deviations at the individual-tree level, they have limited impact on the strength, timing, and stability of climate–growth relationships. Comparison of sites from northern Germany to southern Italy reveal a north-to-south narrowing of climate-sensitive growth periods and a notable increase in sensitivity during the late 20th century. Despite their short-term influences, our findings show that disturbances in old-growth beech forests act only as secondary modifiers rather than primary drivers of climate-growth relationships and thereby justify dendroclimatic reconstructions without prior disturbance adjustment.

1. Introduction

Disturbances are fundamental drivers of forest ecosystem dynamics, exerting strong controls on carbon sequestration, biodiversity, and species composition across global forests (Altman et al., 2024; Reddy et al., 2025). They originate from both natural agents, including wind, drought, wildfire, and insects, and anthropogenic activities such as logging and land-use change (Seidl et al., 2024). Disturbances regulate ecosystem structure, regeneration, and resilience, producing cascading effects on nutrient cycling, habitat availability, and long-term successional trajectories (Johnstone et al., 2016; Seidl et al., 2017; Turner, 2010). In dense, closed-canopy temperate forests, canopy disturbance events are typically associated with branch falls and the death of one or a few individuals, forming canopy "gaps" (Gray et al., 2012). These events define characteristic disturbance regimes characterized by frequency, size, and severity across spatial and temporal gradients (Vacchiano et al., 2017). Whether localized (endogenous) or stand-wide (exogenous), canopy disturbances play a key role in shaping forest composition, structure, and functional processes (Frankovič et al., 2021; Jucker, 2022; Nagel et al., 2014; Reddy et al., 2025). Despite their potential impact on the temperate forest ecotone, assessing how canopy disturbances influence climate-growth relationships has been largely

* Corresponding author.
E-mail address: eziaco@uni-mainz.de (E. Ziaco).

https://doi.org/10.1016/j.dendro.2026.126537
Received 18 March 2026; Received in revised form 14 May 2026; Accepted 18 May 2026
Available online 19 May 2026

neglected, thereby hindering the potential for dendroclimatic and paleoclimatic studies in long-lived temperate forest ecosystems.

European beech (*Fagus sylvatica* L.) is one of Europe's most crucial temperate hardwood species. Its natural distribution extends from Sicily to southern Scandinavia and from the Iberian Peninsula to eastern Europe (ca. 38°N to 60°N, −5° to 28°E) (Leuschner, 2020). It is generally considered reliant on sufficient summer moisture and mild winter temperatures. However, climate warming, coupled with rising evapotranspiration demands, may expose European beech to increasing drought stress, and the growth response to warming appears to be highly site-specific, even at the southern limit of its range (Baliva et al., 2024). A few remaining patches of natural, unmanaged beech forests offer opportunities to study long-term growth dynamics and ecosystem functions (e.g., Adhikari et al., 2024; Piovesan et al., 2005a,b). In these forests, characterized by a high level of naturalness (Di Filippo et al., 2007), gap dynamics represent the prevailing disturbance regime, with frequent low-severity disturbances and occasional major events affecting more than one tree (Ziaco et al., 2012). These stands, therefore, offer a unique baseline for investigating the effects of canopy disturbances on climate sensitivity in beech populations. However, an evaluation of the stability in climate-growth relationships in old-growth beech stands across a broad range of climatic and environmental conditions is still incomplete or missing.

The frequency and severity of past canopy disturbances can be assessed through tree-ring data, providing valuable insights into the environmental history and landscape dynamics (Nagel et al., 2007; Ziaco et al., 2012). The opening of canopy gaps stimulates a growth release in neighboring trees (Reddy et al., 2025), characterized by a sudden and persistent increase in ring width, followed by a gradual decline caused by canopy closure. Tree-ring records can capture these changes within a few years of the disturbance, reflecting the tree's response to reduced competition for light availability and soil resources, enabling the dating of disturbance-driven growth releases (Nowacki and Abrams, 1997; Veblen et al., 1991). By temporarily altering light regimes, nutrient availability (e.g., NH_4^+, NO_3^-, P), and soil biophysical properties (e.g., soil organic carbon content), canopy gaps modify inter- and intra-specific competition dynamics and create microclimatic conditions that differ from those of the surrounding stand (Muscolo et al., 2014; Tong et al., 2024). From a dendroclimatic perspective, these disturbance-driven growth releases constitute noise that can obscure the regional climatic signal recorded in tree rings (Rydval et al., 2018). Consequently, to accurately evaluate forest responses to climatic variability, from both ecological and paleoclimatic perspectives, it is essential to quantify the contribution of disturbance-driven growth fluctuations to the climate sensitivity of ring-width chronologies (Druckenbrod et al., 2024). This is particularly important when disturbances temporarily alter the climatic signal and potentially affect the reliability of dendrochronological climate reconstructions (Martinez del Castillo et al., 2024).

Ring-width series can be used to detect radial growth releases associated with past ecological disturbance events using dendrochronological techniques, building on the fact that abrupt canopy disturbances can be distinguished from climatically driven growth pulses, which are typically associated with slow, constant increases in radial growth (Rubino and McCarthy, 2004). In temperate forests, a flexible approach to detecting radial growth releases associated with canopy disturbances is the boundary line release criteria (Black and Abrams, 2003, 2004), which scale growth releases based on the maximum physiological potential established by prior growth (PG) rates defined for a given species, region, and biogeoclimatic conditions (Ziaco et al., 2012). The boundary line release criteria improve the accuracy of disturbance-related growth release thresholds and the identification of non-climatic release events (Black and Abrams, 2003).

Here, we investigate three old-growth beech forests in northern Germany, central Germany, and southern Italy, all listed as UNESCO World Heritage Sites "Ancient and Primeval Beech Forests of the Carpathians and Other Regions of Europe" (Kirchmeir and Kovarovics, 2020), spanning a wide ecoclimatic gradient to assess how canopy disturbances affect climate sensitivity. After reconstructing disturbance histories for each site and identifying major disturbance-driven growth releases in individual trees, we develop separate chronologies for undisturbed and disturbed individuals to evaluate whether, how, and to what extent canopy disturbances alter the climatic signal encoded in tree-ring width.

2. Material and methods

2.1. Study sites

Tree-ring width (TRW) data were collected in three old-growth European beech (*F. sylvatica* L.) forests distributed along a steep ecoclimatic gradient spanning over 1200 km from northeastern Germany to the southern Apennines in Italy (Fig. 1a, b; Table 1). The northernmost site is the old-growth forest of Serrahn (SER) located in the Müritz National Park (northeastern Germany). Although the area experienced extensive timber extraction during and immediately after World War II (Kaiser et al., 2015), this stand represents one of the most natural lowland beech forests in Central-Northern Europe (von Oheimb et al., 2005). Based on the gridded TerraClimate dataset (Abatzoglou et al., 2018), the mean annual temperature for the period 1991–2020 was 8.9 °C and annual precipitation 581 mm. Temperature and precipitation peak in July (17.9 °C, 79.4 mm), whereas January (0.0 °C) is the coldest month, and February (31 mm) experiences the lowest precipitation (Fig. 1c).

The second site is represented by the old-growth beech forest in Kellerwald (KEL), within the Kellerwald-Edersee National Park. It is the largest contiguous remnant of acidophilous beech forest with wood rush (*Luzula* spp.) in Germany (Adhikari et al., 2025). The mean annual temperature is 8.5 °C, with the highest in July (17.0 °C) and the lowest in January (0.6 °C) (reference period 1991–2020). The average annual precipitation is 869 mm, peaking in July (89 mm) (Fig. 1d). Both SER and KEL are characterized by a predominantly semi-humid to humid, cool-temperate climate (Lauer and Frankenberg, 1988).

The third site is the old-growth beech forest of Pollinello (POL) in the Pollino National Park, in the southern sector of the Apennine mountain range. This forest lies near the southern edge of the species' distribution and represents one of the southernmost components of the UNESCO network of ancient beech forests (Piovesan et al., 2019). During 1991–2020, the mean annual temperature was 8.2 °C, with the highest temperature recorded in August (17.3 °C) and the lowest in February (0.3 °C). Annual precipitation totals 886 mm, with July recording the lowest precipitation (26.8 mm; Fig. 1e). Nevertheless, the high elevation (1970 m a.s.l.) of the study area promotes frequent clouds and orographic fog and precipitation, creating favorable conditions for the growth of a mesic hardwood deciduous forest (Feoli and Lagonegro, 1982).

2.2. Chronology development

The sampling campaign at SER and KEL took place in the summer of 2023. At each site, 50 trees were selected, and two 5-mm wood cores were extracted using a Haglöf increment borer from opposite sides of the stem, yielding 100 cores per site. At POL, we used a total of 94 increment cores collected during several field campaigns between 2015 and 2024 (Table 1). Samples were mounted and sanded with progressively finer sandpaper (up to 1000-grit), scanned with an EPSON Expression 10000XL flatbed scanner at 2400 dpi, and TRW measured using CooRecorder (Cybis Elektronik & Data AB, Saltsjöbaden, Sweden). Cross-dating was verified visually and statistically using COFECHA (Holmes, 1983). The cross-dated series were averaged to produce raw TRW site chronologies.

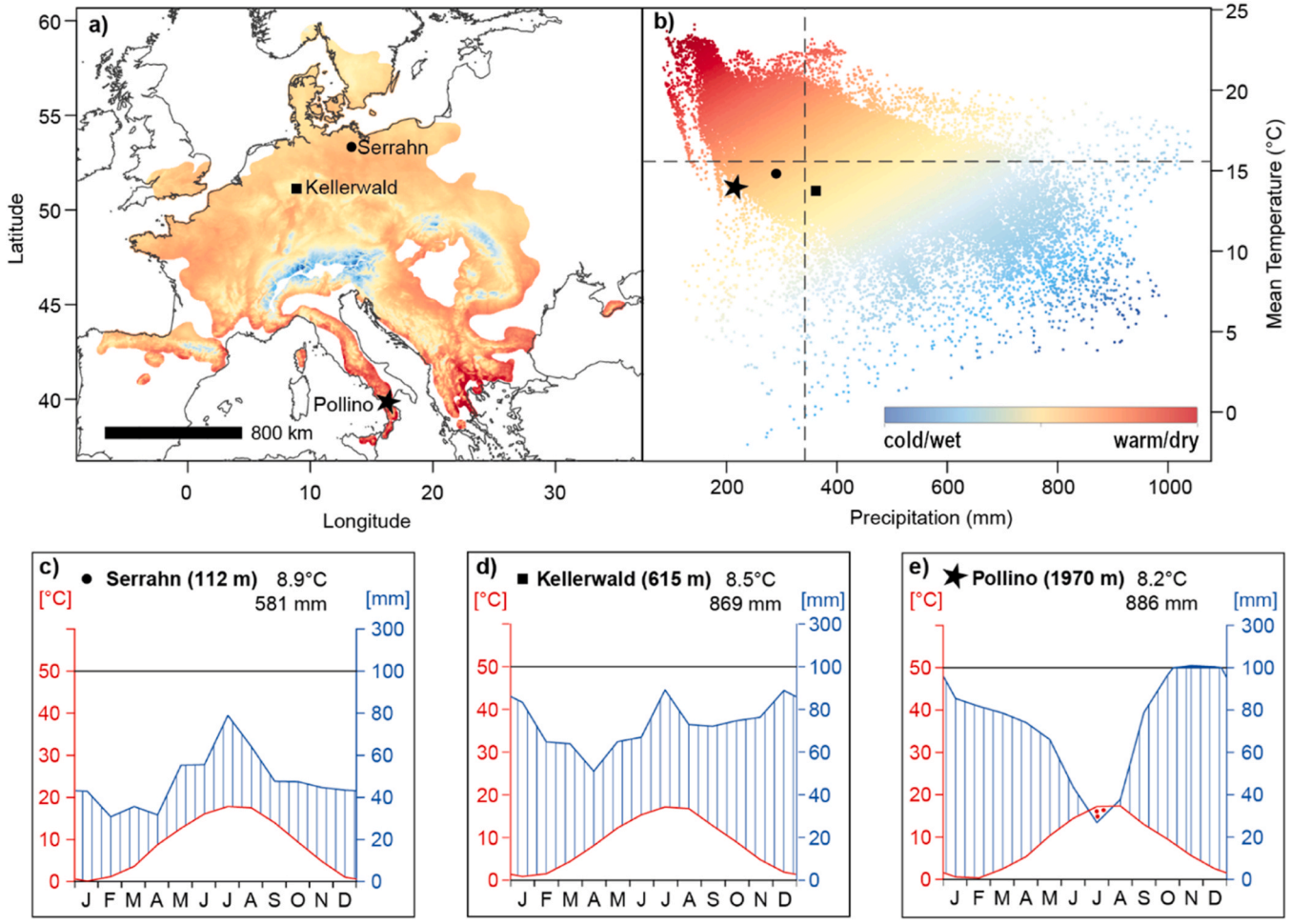

Fig. 1. a) Location and climatic characterization of the study sites Serrahn, Kellerwald (both in Germany), and Pollino (Italy) within the natural distribution range of European beech (*Fagus sylvatica* L.). b) Position of the study sites in the species bioclimatic space. Colors in a and b represent the ratio between April–September mean temperature and precipitation from warm/dry (red) to cold/wet (blue) between 1970 and 2020, based on the WorldClim v2.1 dataset at 2.5 arc-min spatial resolution. Dashed lines in b indicate the median values of the species bioclimatic space. Climate diagrams for Serrahn (c), Kellerwald (d), and Pollino (e) are based on TerraClimate data, whose 4-km spatial resolution provides improved site-level climate characterization, particularly in mountainous terrain.

Table 1
Summary information of the study sites. Empirical measurements of signal strength (Rbar, EPS, SNR) and Ar1 are referred to the 100-yrs spline detrended series.

Site	Lat	Lon	Elevation (m a.s.l.)	Chronology	Cores (n)	Mean Age (years)	Max Age (years)*	Age5 (years) **	Period (n ≥ 10)	Rbar	EPS	SNR	Ar1
Serrahn	53°20'24''N	13°11'52''E	112	all	86	193	305	281	1778–2022	0.51	0.98	44.94	0.52
				undisturbed	24	198	296	262	1818–2022	0.47	0.94	16.58	0.46
				disturbed	62	191	305	265	1798–2022	0.43	0.97	35.25	0.55
Kellerwald	51°07'52"N	8°58'45"E	615	all	79	168	190	187	1839–2022	0.51	0.99	61.87	0.34
				undisturbed	17	169	181	179	1849–2022	0.53	0.94	16.76	0.31
				disturbed	62	168	190	187	1839–2022	0.51	0.98	48.18	0.35
Pollino	39°54'24''N	16°12'10''E	1970	all	94	302	624	570	1549–2022	0.38	0.98	58.60	0.46
				undisturbed	42	264	468	433	1549–2022	0.39	0.97	32.06	0.43
				disturbed	52	333	624	570	1686–2022	0.38	0.96	25.67	0.48

* length of the longest ring-width series
** mean length of the five longest ring-width series

2.3. Detection of disturbance-driven growth releases

To evaluate the effect of canopy disturbances on climate sensitivity of beech across the environmental gradient, we first detected growth releases associated with non-climatic canopy disturbances. To do so, we identified the major radial growth releases in ring-width series using the boundary-line release criteria (BL) (Black and Abrams, 2004) (Supplementary Methods S1). This approach has been widely applied in old-growth beech stands and has proven effective across a broad range of biogeoclimatic conditions (Splechtna et al., 2005; Trotsiuk et al., 2012; Ziaco et al., 2012). The boundary line represents the species' maximum release potential, expressed as percent growth change (GC) at any given level of prior growth (PG). It allows the disentanglement of abrupt true ecological disturbances (i.e., those caused by windthrows) from slow climate-driven radial growth releases. Because high data replication is required to calculate reliable boundary lines

(Black et al., 2009), we integrated the TRW data for the German sites with records from the International Tree-Ring Data Bank (ITRDB), including three sites near SER and four sites near KEL (Tab. S2). The boundary line for Serrahn was based on 33,903 tree rings, while that for Kellerwald comprised 22,941 tree rings. For Pollino (28,428 tree rings), the regional boundary line was calculated solely from the data available in this study, since suitable nearby ITRDB chronologies representing comparable high-elevation old-growth Mediterranean beech conditions were not available.

After detecting individual growth releases, series were detrended over their full length using a cubic smoothing spline with a 50% frequency response cutoff at 100 years (from hereon: 100-year spline) to retain low-frequency variability (Cook and Kairiukstis, 1990), and raw TRW was converted to Ring-Width Indexes (RWI). Empirical measures of signal strength, including interseries correlation (Rbar), expressed population signal (EPS), and signal-to-noise ratio (SNR), were computed to assess the strength of the common signal at each site (Hughes et al., 2011). Finally, the series were merged into several distinct chronologies using a biweight robust mean to mitigate the influence of outliers and further stabilize the variance (Cook and Kairiukstis, 1990). First, a site chronology, including all series, was developed, hereafter referred to as *all*. To disentangle the impact of disturbances on the climatic signal, two additional chronologies were created for each site, one for *undisturbed* series (i.e., individual ring-width series that had not experienced any major disturbance-driven growth releases) and one for *disturbed* series (i.e., ring-width series with at least one disturbance-driven growth release).

2.4. Climate data and statistical analysis

For both disturbed and undisturbed series, we tested relationships between growth and monthly climatic parameters, including maximum temperature (Tmax), total precipitation (Ppt), diurnal temperature range (DTR), cloud cover (CC) and the 3-month Standardized Precipitation-Evapotranspiration Index (SPEI). Tmax, Ppt, DTR, and CC were extracted from the gridded 0.5° CRU TS v.4.08 dataset (Harris et al., 2020), while the 3-month SPEI was obtained from the Global SPEI database (Vicente-Serrano et al., 2010). In addition, monthly vapor pressure deficit (VPD) values were calculated for each site using gridded mean temperature and relative humidity data from the E-OBS dataset (Cornes et al., 2018). Climate-growth relationships were investigated by correlating RWI with monthly Tmax, Ppt, SPEI, CC, and DTR data from 1902 to 2022, including previous year June to current year September. To ensure consistency between biological and environmental signals, all monthly series of climatic variables were detrended using a 100-year spline, matching the applied detrending to the tree-ring width series (Ols et al., 2023). Because VPD records were available only for the period 1962–2022, all climate-growth relationships were additionally assessed for this period for comparison. A Fisher's *Z*-test was performed to assess whether the correlations between the two time periods differ significantly. The temporal stability of dendroclimatic correlations was evaluated using bootstrapped Pearson correlation coefficients (Guiot, 1991), computed with a 31-year moving window, shifted by one year at a time, between indexed site chronologies and climate variables. Numerical computations were performed in the R software environment (R Core Team, 2024) using the packages dplR (Bunn, 2008) for detrending, chronology construction, and correlation analyses, and TRADER (Altman et al., 2014) for detecting growth releases and constructing disturbance histories. VPD calculations were performed using the *plantecophys* package (Duursma, 2015).

3. Results

3.1. Chronology statistics

The oldest trees were found at POL, where maximum and mean tree ages reach 624 and 302 years, respectively (Table 1). In contrast, the northern sites are younger, with maximum (mean) ages of 305 (193) years at SER and 190 (168) years at KEL. Due to wood quality, not all growth series could be absolutely dated. At SER, 86 of the 100 series were successfully crossdated. The resulting *undisturbed* chronology comprises 24 series and spans 1818–2022 ($n \geq 10$), with a mean tree age of 198 years. The *disturbed* chronology includes the remaining 62 series spanning 1798–2022, with an average age of 191 years (Fig. 2a; Table 1). At KEL, 79 series were successfully crossdated. The *undisturbed* chronology ($n = 17$) extends from 1849 to 2022, with a mean age of 169 years, while the *disturbed* chronology ($n = 62$) spans 1839–2022, with an average age of 168 years (Fig. 2b; Table 1). The oldest chronologies were developed at POL, where 94 series were crossdated. The *undisturbed* chronology ($n = 42$) covers 1549–2022, and the *disturbed* chronology ($n = 52$) extends from 1686 to 2022 (Fig. 2c; Table 1).

Radial growth in both German beech forests is nearly twice as high as that observed at POL. Particularly notable is the elevated growth rate for *disturbed* trees at SER, which exceeded 3 mm/year for five consecutive years (1941–1945), whereas the maximum growth rate of *undisturbed* trees was 2.1 mm/year during the same period. Average growth rates calculated for non-overlapping 50-year age classes reveal higher mean growth and greater variability at SER and KEL than at POL. At SER (KEL), growth ranges from 0.72 to 1.63 mm yr^{-1} (1.08–1.43 mm yr^{-1}) in undisturbed trees and from 0.92 to 2.00 mm yr^{-1} (1.23–1.55 mm yr^{-1}) in disturbed trees. In contrast, at POL, values are lower, ranging from 0.45 to 0.79 mm yr^{-1} in undisturbed trees and from 0.52 to 0.98 mm yr^{-1} in disturbed trees (Fig. S2). Across all sites, descriptive statistics (Table 1) for *undisturbed* chronologies show slightly higher Rbars (SER = 0.47, KEL = 0.53, and POL = 0.39) than for *disturbed* records (SER = 0.43, KER = 0.51, and POL = 0.38). EPS ranges from 0.94 to 0.98 and exceeds the standard threshold of 0.85 (Wigley et al., 1984) in all cases. Ar1 values range from 0.31 to 0.55 and are consistently slightly higher in *disturbed* series compared to *undisturbed* series (Table 1; Fig. S1).

To assess the degree of similarity and shared variance between the paired chronologies, we calculated the correlation coefficients between *undisturbed* and *disturbed* chronologies at each site for the 1902–2022 period. The chronologies exhibited high synchrony across all sites, indicating a strong common response to regional environmental drivers. At SER, the correlation between *undisturbed* and *disturbed* chronologies was $r = 0.93$. Similarly high levels of agreement were found at KEL ($r = 0.96$) and POL ($r = 0.96$) (all $p < 0.001$).

3.2. Regional boundary lines and disturbance history

Site-specific differences in growth-release dynamics are evident in the form and magnitude of the fitted boundary lines. At SER, the boundary line was described by a log-linear mixed function, whereas at KEL and POL, a linear exponential function provided the best fit (Table S1; Fig. S3). Overall, SER shows greater release potential than KEL and POL, particularly for PG > 0.5 mm yr^{-1} . For example, at a PG of 2 mm yr^{-1} , beech trees at SER have a maximum release potential (i.e., growth change) of 161%, whereas at KEL and POL it is only 60% and 50%, respectively. However, for PG < 0.5 mm yr^{-1} , trees at KEL show higher release potential than at SER (Fig. S3). Among all sites, POL exhibits the highest release potential for low PG values (< 0.5 mm yr^{-1}).

Between 1729 and 2007, 89 major growth releases were identified at SER, occurring in 64 of 84 series. The highest disturbance frequencies, based solely on the disturbance onset year, were observed in 1875 and 1920, when 17% and 16.7% of the series, respectively, exhibited a release event (Fig. 3a). Elevated disturbance activity was also evident from the 1930s to the 1940s, with an average of 8% of the series showing release events. In contrast, several periods without any detected releases were observed, most notably a 30-year interval between 1820 and 1850. At KEL, 106 major disturbances were detected between 1844 and 2012, affecting 41 of 79 series (Fig. 3b). Disturbance frequency peaked in 1915 at 24.5% of the series and again between 1960 and 1990, with detected

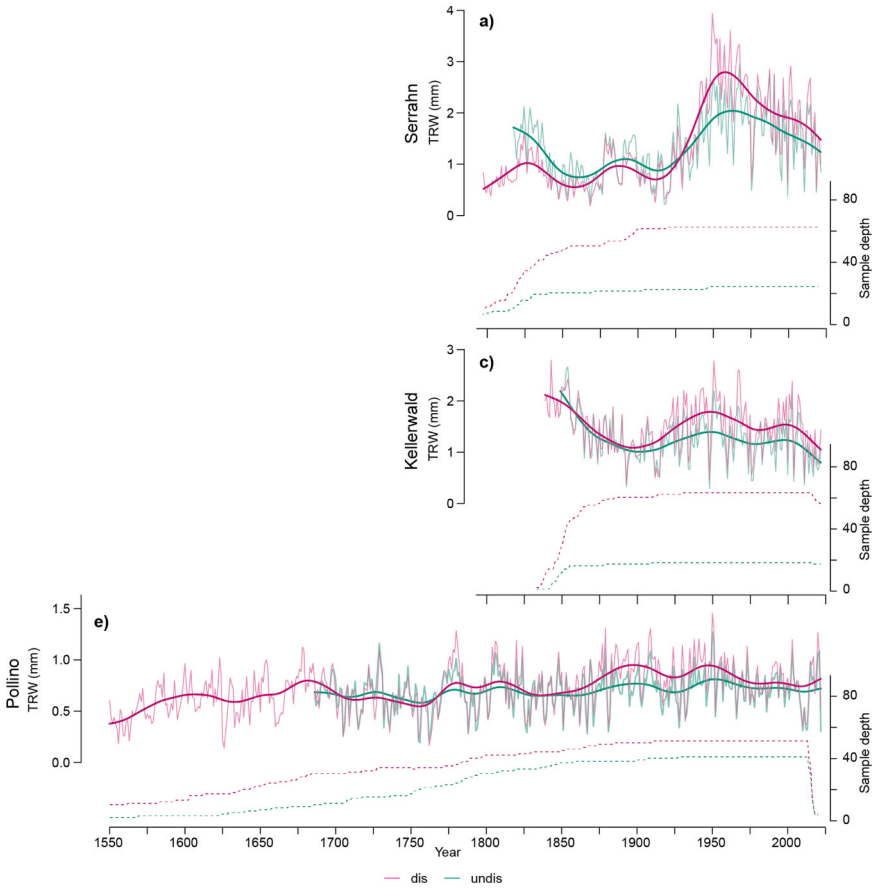

Fig. 2. Raw TRW chronologies (n ≥ 10) of undisturbed (green) and disturbed trees (purple) in Serrahn (a), Kellerwald (b), and Pollino (c). Dashed curves show sample replication back to a minimum of 10 series. Bold curves are 50-year splines.

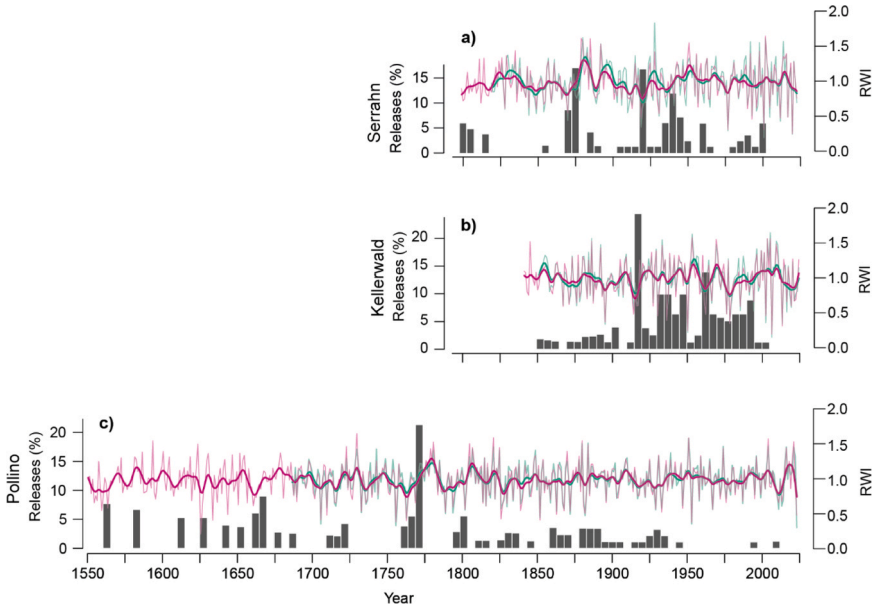

Fig. 3. Standardized undisturbed (green) and disturbed (purple) TRW chronologies for Serrahn (a), Kellerwald (b), and Pollino (c), along with detected major disturbances. The histogram displays the ratio between disturbed and all series in percent in 5-year intervals. Bold curves are 10-year splines.

releases in 5–14% of the series. By comparison, fewer events were detected at POL over the period 1406–2005, with 79 major disturbances occurring in 52 of 94 series (Fig. 3c). The most pronounced peak occurred in the 1770 s, when release events were identified in 21.3% of the ring-width series. Similar to SER, several periods without detected release events were evident, most notably around 1600, between 1725 and 1755, from 1775 to 1790, and between 1950 and 1995.

3.3. Climate-growth relationships

3.3.1. Static dendroclimatic signals

Across all sites, dendroclimatic analyses revealed significant climate–growth relationships over the full period (1902–2022), with tree growth responding predominantly to previous-year climatic conditions, particularly during summer. The strength and timing of these relationships varied among sites and climate variables, but were broadly consistent across all types of chronologies.

At the northern sites, RWI showed a significant negative response to previous-year Jul–Sep Tmax. At SER, correlations were r = -0.49 for *undisturbed*, r = -0.42 for *disturbed*, and r = -0.45 for *all* trees (Fig. 4a). At KEL, the same response window was observed, with similar correlations for *undisturbed* (r = -0.38), *disturbed* (r = -0.37), and *all* trees (r = -0.37; Fig. 4d). In the recent period (1962–2022), Tmax sensitivity remained broadly stable at SER and KEL. At POL, Tmax responses were more variable: during the full period, all chronologies showed a negative response to current-year April Tmax (r = -0.22), whereas the recent period was characterized by stronger negative correlations with previous-year summer Tmax, from Jun–Sep for *undisturbed* and *all* trees, and Jul–Aug for disturbed trees (Fig. 4g). However, Fisher's Z tests indicated that these seasonal differences between periods were not

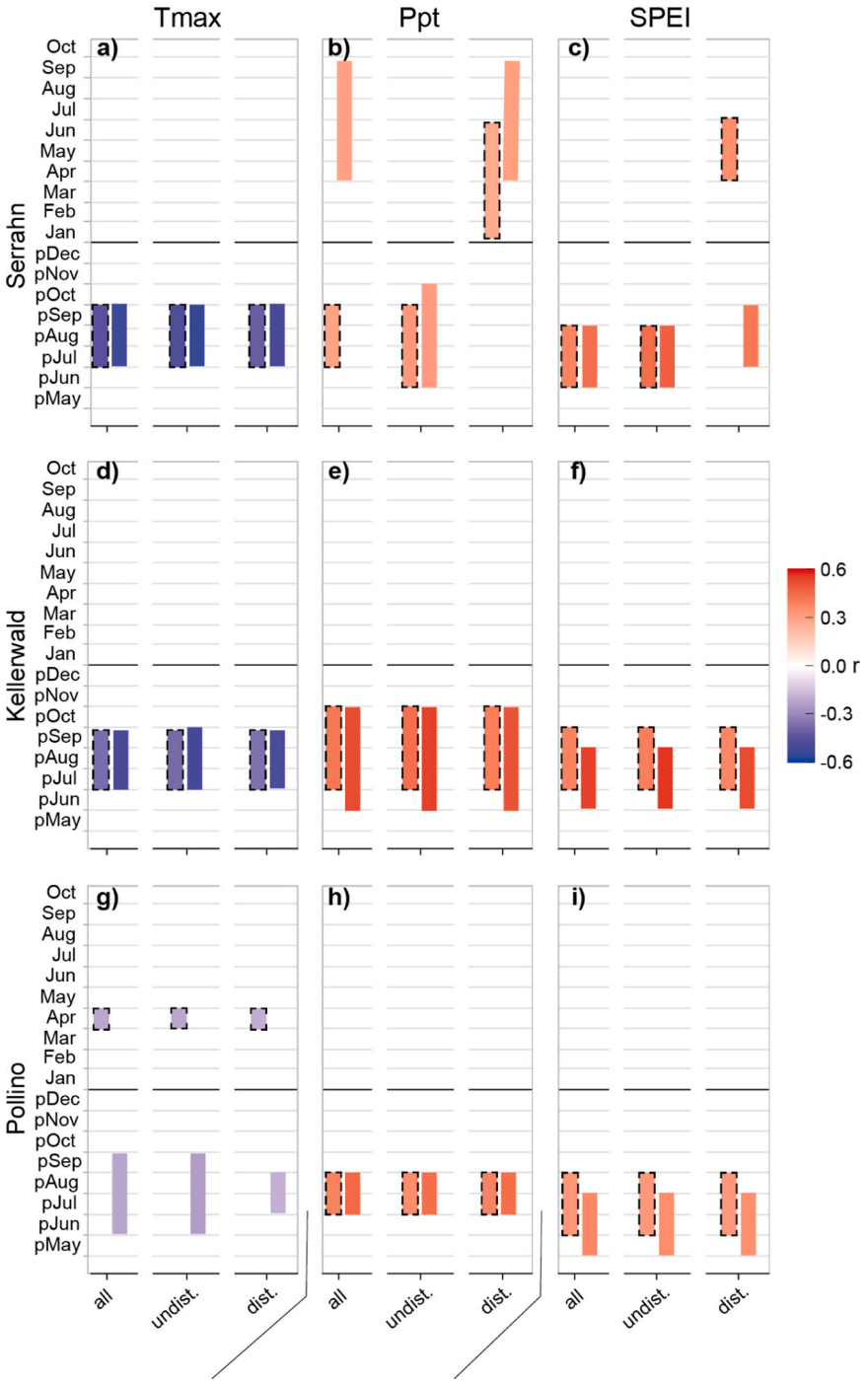

Fig. 4. Monthly correlations between the standardized Serrahn, Kellerwald, and Pollino chronologies and maximum temperature (Tmax; a, d, g), precipitation (Ppt; b, e, h), and the Standardized Precipitation Evapotranspiration Index (SPEI; c, f, i) from previous-year May to current-year October. Dashed-bordered bars represent the full period 1902–2022, while open bars represent the period 1962–2022.

statistically significant.

Growth responses to precipitation and SPEI were consistently positive and mainly associated with previous-year moisture conditions. At SER, *undisturbed* trees responded to previous Jun–Sep Ppt (r = 0.32), *disturbed* trees to current Jan–Jun Ppt (r = 0.27), and *all* trees to previous Jul–Sep Ppt (r = 0.29; Fig. 4b). At KEL, all chronologies showed positive correlations with previous Jul–Oct Ppt, with r = 0.44 for *undisturbed*, r = 0.41 for *disturbed*, and r = 0.42 for *all* trees (Fig. 4e). At POL, the response was centered on previous Jul–Aug Ppt and was highly consistent among chronologies, with r = 0.37, r = 0.38, and r = 0.39 for *undisturbed*, *disturbed*, and *all* trees, respectively (Fig. 4h). SPEI correlations showed comparable patterns. At SER, *undisturbed* and *all* trees responded positively to previous Jun–Aug SPEI (r = 0.45 and r = 0.36), whereas *disturbed* trees correlated most strongly with current Apr–Jun SPEI (r = 0.38; Fig. 4c). At KEL, RWI was positively related to previous Jul–Sep SPEI across chronologies, with r = 0.40, r = 0.37, and r = 0.38 for *undisturbed*, *disturbed*, and *all* trees, respectively (Fig. 4f). At POL, growth responded positively to previous Jun–Aug SPEI (r = 0.32; Fig. 4i). In the recent period, precipitation and SPEI response windows showed minor adjustments, but Fisher's Z tests confirmed that these variations did not represent significant shifts in climate sensitivity.

Variables related to atmospheric demand and radiation showed

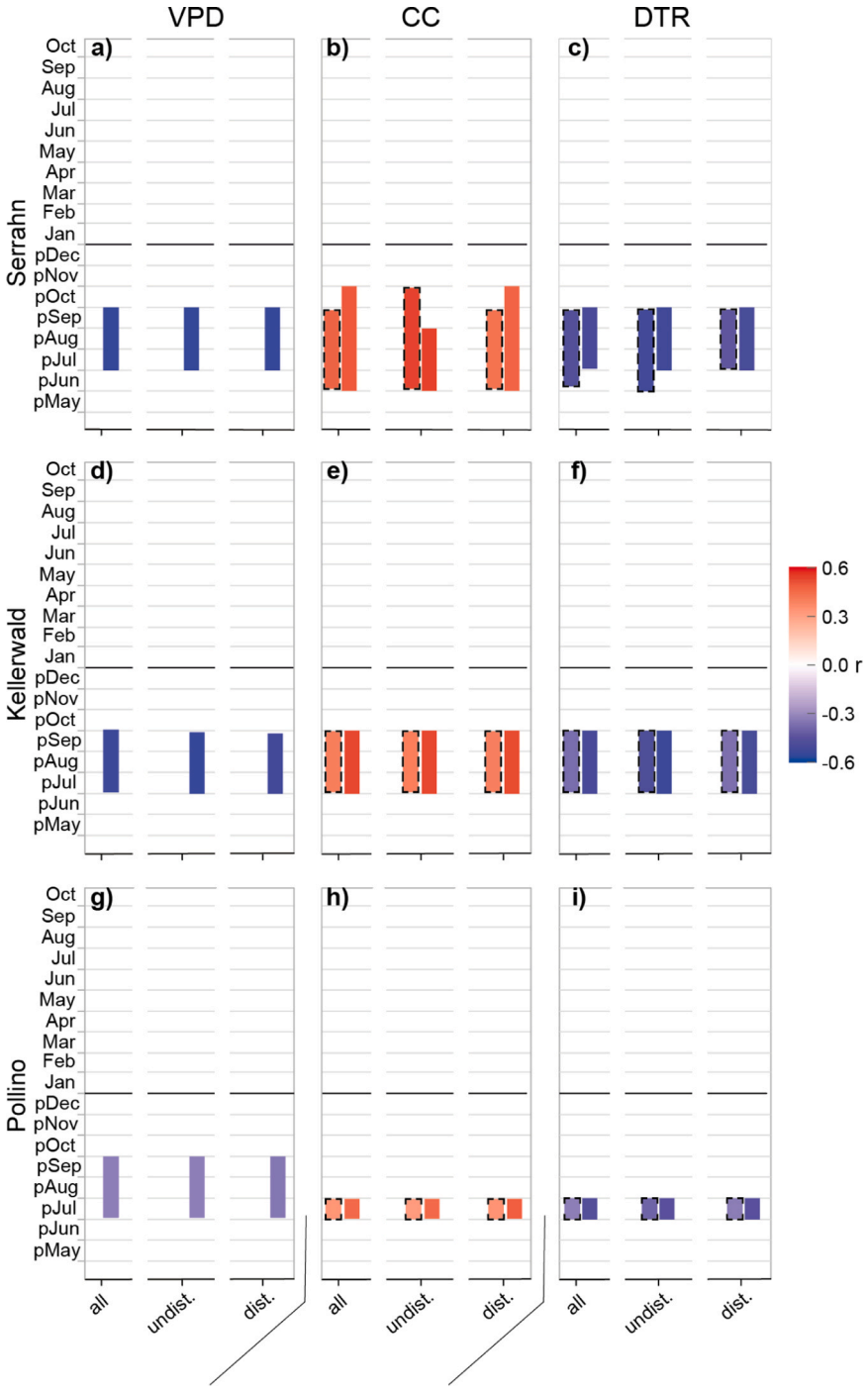

Fig. 5. Monthly correlations between the standardized Serrahn, Kellerwald, and Pollino chronologies and vapor pressure-deficit (VPD; a, d, g), cloud cover (CC; b, e, h), and diurnal temperature range (DTR; c, f, i) from previous-year May to current-year October. Dashed-bordered bars represent the full period 1902–2022, while open bars represent the period 1962–2022.

complementary patterns. VPD had a negative effect on growth during the recent period, with the strongest correlations centered on previous Jul–Sep. This signal was particularly pronounced at SER and KEL (r = -0.54), and weaker at POL (r = -0.33; Fig. 5a, d, g). Cloud cover was positively associated with growth, again mainly during the previous summer. At SER, *undisturbed* trees correlated with previous Jun–Oct CC (r = 0.53), whereas *disturbed* and *all* trees responded to previous Jun–Sep CC (r = 0.38 and r = 0.42; Fig. 5b). At KEL, previous Jul–Sep CC influenced all chronologies similarly (r = 0.40; Fig. 5e). At POL, growth responded positively to previous July CC, with r = 0.31, r = 0.34, and r = 0.33 for *undisturbed*, *disturbed*, and *all* trees, respectively (Fig. 5h). The recent period showed only slight seasonal variations at SER, while response windows at KEL and POL remained stable; none of these differences were statistically significant.

DTR was negatively correlated with growth at all sites. At SER, undisturbed trees responded to previous Jun–Sep DTR (r = -0.52), whereas *disturbed* and *all* trees responded to previous Jul–Sep DTR (r = -0.44 and r = -0.47; Fig. 5c). At KEL, the negative response was consistently centered on previous Jul–Sep DTR across chronologies, with r = -0.38, r = -0.37, and r = -0.38 for *undisturbed*, *disturbed*, and *all* trees, respectively (Fig. 5f). At POL, all chronologies responded negatively to previous July DTR, with r = -0.40 for *undisturbed*, r = -0.33 for *disturbed*, and r = -0.33 for *all* trees (Fig. 5i). During 1962–2022, only SER showed slight variation in the DTR response window, whereas all other chronologies maintained stable seasonal patterns.

Overall, climate-growth correlations were slightly stronger during 1962–2022 than during 1902–2022 for several variables and sites (Table 2). However, Fisher's Z tests showed that these differences, as well as the apparent variations in seasonal response windows, were generally non-significant (Tab. S3).

3.3.2. Temporal stability

The analysis of the temporal stability of static climatic correlations revealed contrasting patterns across sites and disturbance conditions. At SER, the relationship between RWI and Tmax (pJul-pSep) shows a strong temporal stability in both *undisturbed* and *disturbed* series, with the relationship strengthening over time (Fig. 6a). Despite different response periods (pJun–pSep/Jan–Jul), the Ppt signal in SER shows only slight variation and remains stable throughout the record. Likewise, the correlation with SPEI exhibits comparable temporal stability for *undisturbed* (pJun–pAug) and *disturbed* (Apr–Jun) trees, despite their differing response windows. After 1995, the temporal development of the SPEI-growth correlations diverges, when correlation values for *disturbed* trees show a modest increase, while the signal for un*disturbed* trees remains stable. CC and DTR both show relatively stable signals over time, being slightly stronger in *undisturbed* than in *disturbed* trees (Fig. 6b). In KEL, the temporal stability analysis reveals similar relationships between TRW and both Ppt and SPEI (Fig. 6c). The Ppt signal remains relatively stable until the 1970s, after which the correlation increases modestly. The relationship with SPEI is weaker than with Ppt until the 1960s and begins to strengthen around 1945, following a comparable positive trend. The signal related to Tmax develops similarly but shows a more pronounced increase in strength over time. The relationships between TRW and both CC and DTR in KEL exhibit similar patterns, with signal strength gradually increasing over time (Fig. 6d).

Running correlations between TRW and both Ppt and SPEI in POL indicate a generally stable climate-growth relationship over time (Fig. 6e). Beginning in the 1980s, however, the correlation with Ppt shows a slight increase in signal strength for both *undisturbed* and *disturbed* trees. In contrast, the Tmax signal exhibits the most significant variability over time. Correlations with CC and DTR exhibit temporal patterns similar to those observed in KEL, with signal strength increasing

Table 2
Main monthly correlations between the standardized Serrahn, Kellerwald, and Pollino chronologies and the climatic parameters.

Site	Chronology	Period	Tmax	Ppt	SPEI	DTR	CC	VPD
Serrahn	undisturbed	1902–2022	-0.49 (pJul–pSep)	0.32 (pJun–pSep)	0.45 (pJun–pAug)	-0.52 (pJun–pSep)	0.53 (pJun–pOct)	-
		1962–2022	-0.56 (pJun–pSep)	0.31 (pJun-pOct)	0.48 (pJun–pAug)	-0.53 (pJul–pSep)	0.54 (pJun–pAug)	-0.56 (pJul–pSep)
	disturbed	1902–2022	-0.42 (pJul–pSep)	0.27 (cJan–cJun)	0.36 (cApr–cJun)	-0.44 (pJul–pSep)	0.43 (pJun–pSep)	-
		1962–2022	-0.50 (pJun–pSep)	0.30 (cApr–cSep)	0.41 (pJul–pSep)	-0.49 (pJul–pSep)	0.46 (pJun–pOct)	-0.54 (pJul–pSep)
	all	1902–2022	-0.45 (pJul–pSep)	0.29 (pJul–pSep)	0.38 (pJun–pAug)	-0.47 (pJul–pSep)	0.46 (pJun–pSep)	-
		1962–2022	-0.53 (pJun–pSep)	0.29 (cApr–cSep)	0.43 (pJun–pAug)	-0.51 (pJul–pSep)	0.49 (pJun–pOct)	-0.55 (pJul–pSep)
Kellerwald	undisturbed	1902–2022	-0.38 (pJul–pSep)	0.44 (pJul–pOct)	0.40 (pJul–pSep)	-0.39 (pJul–pSep)	0.40 (pJul–pSep)	-
		1962–2022	-0.51 (pJun–pSep)	0.55 (pJun–pOct)	0.56 (pJun–pAug)	-0.53 (pJul–pSep)	0.53 (pJul–pSep)	-0.54 (pJul–pSep)
	disturbed	1902–2022	-0.37 (pJul–pSep)	0.41 (pJul–pOct)	0.37 (pJul–pSep)	-0.37 (pJul–pSep)	0.39 (pJul–pSep)	-
		1962–2022	-0.49 (pJun–pSep)	0.50 (pJun–pOct)	0.52 (pJun–pAug)	-0.49 (pJul–pSep)	0.53 (pJul–pSep)	-0.52 (pJul–pSep)
	all	1902–2022	-0.37 (pJul–pSep)	0.42 (pJul–pOct)	0.38 (pJul–pSep)	-0.38 (pJul–pSep)	0.40 (pJul–pSep)	-
		1962–2022	-0.50 (pJun–pSep)	0.52 (pJun–pOct)	0.53 (pJun–pAug)	-0.50 (pJul–pSep)	0.53 (pJul–pSep)	-0.53 (pJul–pSep)
Pollino	undisturbed	1902–2022	-0.22 (cApr)	0.36 (pJul–pAug)	0.32 (pJun–pAug)	-0.40 (pJul)	0.31 (pJul)	-
		1962–2022	-0.24 (pJun-pSep)	0.44 (pJul–pAug)	0.36 (pMay–pJul)	-0.45 (pJul)	0.45 (pJul)	-0.33 (pJul–pSep)
	disturbed	1902–2022	-0.20 (cApr)	0.38 (pJul–pAug)	0.32 (pJun–pAug)	-0.33 (pJul)	0.34 (pJul)	-
		1962–2022	-0.20 (pJul-pAug)	0.44 (pJul–pAug)	0.35 (pMay–pJul)	-0.45 (pJul)	0.49 (pJul)	-0.35 (pJul–pSep)
	all	1902–2022	-0.22 (cApr)	0.39 (pJul–pAug)	0.33 (pJun–pAug)	-0.33 (pJul)	0.33 (pJul)	-
		1962–2022	-0.23 (pJun-pSep)	0.45 (pJul–pAug)	0.37 (pMay–pJul)	-0.46 (pJul)	0.47 (pJul)	-0.33 (pJul–pSep)

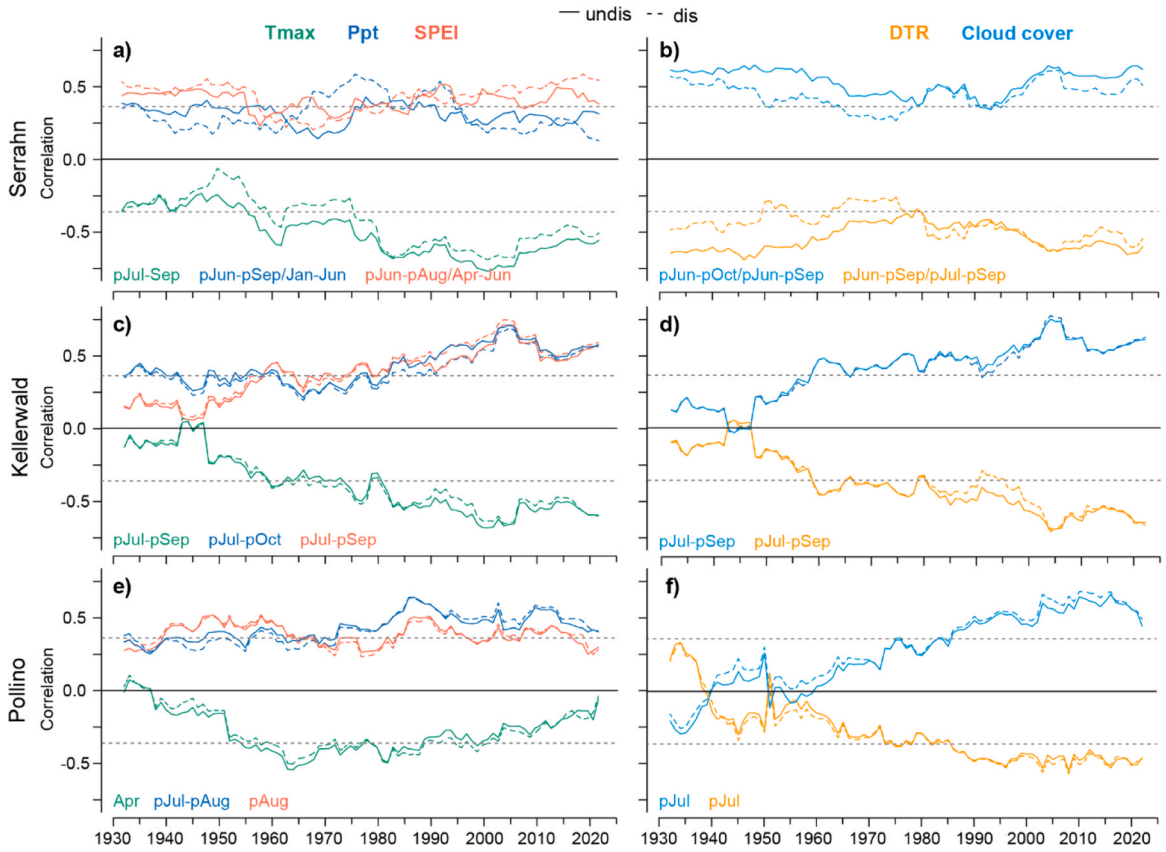

Fig. 6. 31-year moving correlations between leading climatic variables with undisturbed (solid) and disturbed (dashed) chronologies from Serrahn (a, b), Kellerwald (c, d), and Pollino (e, f) from 1902 to 2022. Green curve is maximum temperature (Tmax), blue precipitation (Ppt), red the Standardized Precipitation Evapotranspiration Index (SPEI), light blue cloud cover, and orange the diurnal temperature range (DTR). Corresponding response periods are color-coded. When different, they are arranged undisturbed/disturbed. Dashed lines indicate $p < 0.05$.

for both parameters (Fig. 6 f).

4. Discussion

The three study sites are characterized by a high degree of naturalness, resulting from decades of little to no human intervention, but differ in stand age and span a broad ecoclimatic gradient (Kirchmeir and Kovarovics, 2020). The German sites exhibit a declining growth trend in recent decades, consistent with previous studies from central and northern Europe (e.g., Martinez del Castillo et al., 2022). Interestingly, the Italian population has maintained a stable growth trend over the last 50 years. This occurs despite its location near the southern geographical distribution limit and its high mountain environment, which exposes trees to harsher conditions such as a shortened growing season and high daily temperature fluctuations. This pattern contrasts with studies reporting declines in growth in the southern range in the last decades (Martinez del Castillo et al., 2022). However, recent observations have shown mixed growth trajectories for beech stands in southern Italy, with Pollino being characterized by an oscillating behavior (Colangelo et al., 2021; Baliva et al., 2024).

All three forests exhibited frequent variation in average growth dynamics, a pattern typical of old-growth forests, indicating that individual trees experienced repeated periods of release and suppression (Piovesan et al., 2003). This resulted in decades with few disturbance events alternating with periods of high disturbance frequency. Interestingly, the periods of major releases concentrated in the second half of the 18th century coincide with those reported for old-growth beech forests in Abruzzo, suggesting a climatic phase characterized by a higher frequency of storms (Ziaco et al., 2012). This pattern is consistent with the disturbance regimes of natural beech forests, in which storms are the primary disturbance agent (Pettit et al., 2021; Vacchiano et al., 2017; Ziaco et al., 2012).

Although canopy disturbances introduce short-term growth increase in old-growth beech forests, our results demonstrate that their impact on climate–growth relationships is negligible. Across sites, climate-growth relationships consistently highlighted moisture availability, both atmospheric and edaphic, as a dominant limiting factor for radial growth, in both disturbed and undisturbed trees. Precipitation, SPEI, and cloud cover had a positive effect on tree growth at all sites, while temperatures, vapor-pressure deficits, and temperature ranges reduced growth, particularly during the previous summer and early autumn, indicating strong carry-over effects. These relationships align well with findings from central and southern Europe (see e.g., Cavin and Jump, 2017; Harvey et al., 2020; Lebourgeois et al., 2005; Piovesan et al., 2005b; Roibu et al., 2022; van der Maaten, 2012) and reflect the sensitivity of European beech to summer drought and heat stress (Leuschner, 2020; Serrano-Notivoli et al., 2025).

Canopy disturbances do not affect individual trees at the same time, so their impact, if any, on the climatic sensitivity of trees is attenuated over time. Differences between *undisturbed* and *disturbed* series, when combined into a chronology, were generally minor in both static and temporal analyses, indicating that long-term climatic forcing outweighs disturbance effects at decadal scales. Only a few exceptions to this pattern were observed. At SER, for example, *disturbed* trees showed stronger correlations with current-year moisture conditions, whereas *undisturbed* trees were more sensitive to previous-year climate signals. This divergence likely reflects legacy effects of intensive timber extraction during and after World War II (Kaiser et al., 2015), which altered stand structure and local microclimate by opening canopies and reducing competition (Abd Latif and Blackburn, 2010). Reduced

competition may favor shallower rooting strategies, increasing dependence on immediate water availability and vulnerability to drought (Mausolf et al., 2018). Despite minor differences in temporal correlations between *disturbed* and *undisturbed* trees, these findings reinforce the conclusion that site-level climate conditions exert a stronger control on growth sensitivity than disturbance history alone (Bosela et al., 2018).

Despite stand history and disturbance frequency, moisture-related control of beech growth was temporally unstable. Instead, climate–-growth correlations strengthened markedly during the second half of the 20th century for both *undisturbed* and *disturbed* trees, coinciding with a major climatic transition towards higher atmospheric water demand across Europe. Following several decades of "global dimming" (ca. 1950–1980), characterized by reduced surface solar radiation due to elevated aerosol loads, a shift toward "global brightening" began in the late 1970s to early 1980s (Wild, 2009; Wild et al., 2005). This transition, driven by declining aerosol emissions after the introduction of air-quality regulations, was accompanied by rising temperatures, increasing vapor-pressure deficits, and more frequent and intense summer droughts (Esper et al., 2024; Ionita and Nagavciuc, 2021; Reid et al., 2016; Toreti et al., 2019). Central and southern Europe experienced a pronounced decline in summer precipitation and soil moisture, whereas winters became wetter and milder (Spinoni et al., 2015). Climate warming intensified evaporative demand and increased the likelihood of physiological drought stress in temperate broadleaf species, mainly European beech (Leuschner, 2020).

Against this background, the strengthening of climate sensitivity in both *undisturbed* and *disturbed* chronologies at KEL and POL beginning in the 1970s, and the emergence of a pronounced maximum temperature signal at SER during the 1980s to mid-2000s, indicate an increasingly dominant climatic control on radial growth. These temporal changes suggest that moisture availability not only governs spatial patterns of growth sensitivity but has also become progressively more limiting over recent decades (Babst et al., 2019; Friedrichs et al., 2009; Li et al., 2024).

At SER and KEL, the pronounced negative response to previous summer maximum temperature, observed in both *undisturbed* and *disturbed*, likely reflects drought-induced carbon limitation and the effects of reproductive dynamics, particularly masting events. High summer temperatures and solar radiation are known cues for mast initiation (Piovesan and Adams, 2001; Hacket-Pain et al., 2025; Journé et al., 2024). These events redirect a substantial portion of assimilates toward seed production, often at the expense of radial growth, as trees prioritize reproduction over storage and stem increment (Hacket-Pain et al., 2018; Müller-Haubold et al., 2013; Selås et al., 2002). The resulting carbon depletion can suppress subsequent growth by reducing available reserves for cambial activity. Thus, the negative correlations with previous summer temperature may reflect both direct physiological stress from heat and indirect legacy effects from mast-related carbon allocation (Dorado-Liñán et al., 2017; Roibu et al., 2022). Interestingly, at POL, growth is negatively impacted by maximum temperature in April. This suggests that higher temperatures during this period may trigger earlier leaf unfolding, which subsequently increases the vulnerability of young tissues to late frost events (Piovesan et al., 2005; Vitasse et al., 2019). Such frost damage to the initial foliage can lead to a significant reduction in photosynthetic capacity and a depletion of non-structural carbohydrate reserves, ultimately resulting in reduced radial growth for the year (Zohner et al., 2020).

The long-term climatic sensitivity, as well as its temporal development at KEL, is particularly strong, given its comparatively moderate climate and high summer precipitation. Our results suggest that beech populations in Central Europe, a region characterized by high climate sensitivity despite its central location in the species` natural distribution, are showing intensified responses to warming and evaporative demand. While these populations represent the core of the European distribution, they exhibit strong water-balance sensitivity, particularly during the growing season (May to June) (Klesse et al., 2024). The pronounced strengthening of drought- and temperature-related signals observed at this site likely reflects a physiological response to recent climatic shifts, even though the long-term correlation with precipitation has remained relatively stable (Fig. 6).

At POL, growth responses reveal a contrasting mechanism in the high mountain Mediterranean environment. While relationships with summer precipitation and SPEI remain relatively stable over time, sensitivity to diurnal temperature range and cloud cover increased markedly, consistent with the long-term analysis showing a narrow response window at this southern site. These findings suggest that under regularly dry summer conditions, growth becomes increasingly constrained by energy balance rather than water input alone. Increased cloud cover reduces incoming solar radiation, lowers evaporative demand, and moderates day–night temperature fluctuations, thereby creating diffuse light and periods of climatically favorable conditions for radial growth (Hughes et al., 2024). However, some caution in interpreting early results (before 1950) is warranted, as historical cloud cover data, especially in mountainous regions, often carry higher uncertainty due to sparse pre-satellite observations.

Analyses of cloud cover and DTR across sites reveal a consistent north-to-south narrowing of climatically relevant response windows. Growth at the northern sites responds to several consecutive summer months, whereas at the southern distribution limit, it is primarily associated with a single dominant month. This spatial pattern, together with the temporal strengthening of climate signals, indicates that increasing climatic limitation restricts growth to progressively shorter periods of favorable conditions toward the southern distribution limit. However, direct observations of xylogenesis or dendrometer data would be valuable to confirm the intra-annual timing of these mechanisms and the precise duration of the growing season.

5. Conclusion

Our results show that canopy disturbance history does not substantially alter the climate sensitivity of radial growth in old-growth beech forests. Although disturbance-driven growth releases introduce pronounced short-term variability in individual tree-ring series, their effects on the strength, timing, and temporal stability of climate-growth relationships are limited. Across sites and climatic gradients, both *disturbed* and *undisturbed* chronologies preserve coherent and ecologically meaningful climate signals, indicating that past disturbances did not fundamentally disrupt the climatic information encoded in beech ring widths. From a dendroclimatic perspective, these findings suggest that *a priori* exclusion of disturbed series from climate reconstructions is unnecessary, particularly in old-growth stands dominated by gap dynamics. Disturbed trees display climate sensitivities comparable to those of undisturbed trees when included in a site chronology, with only minor differences in response timing and seasonality. Although disturbance-driven growth pulses can locally alter variance and introduce short-term departures from mean growth trends, they do not systematically weaken climate correlations or produce persistent biases in long-term climate signals when appropriate standardization and chronology-building techniques are applied (Bontemps and Esper, 2011; Cook and Kairiukstis, 1990).

Importantly, our analyses indicate that including disturbed trees may enhance the representation of climate variability by increasing sample depth and capturing a broader range of microclimatic conditions, particularly for variables related to atmospheric moisture demand and radiation (VPD, cloud cover, and DTR), which emerged as the strongest growth controls across sites. For paleoclimate studies using European beech, often considered a species with weak or inconsistent climate sensitivity (Diers et al., 2023), our results demonstrate that robust climate signals can be recovered when spatial gradients, temporal non-stationarity, and disturbance effects are accounted for. As disturbances have also likely influenced tree-ring series derived from historical or subfossil material used to extend chronologies over centuries to

millennia, studying disturbed living trees may provide important reference information for interpreting long-term chronologies. Rather than excluding disturbed trees *a priori*, we advocate for their careful environmental evaluation and contextual integration, particularly in old-growth forests where disturbance is an intrinsic component of ecosystem dynamics. Disturbance effects that appear muted in ring-width chronologies may nonetheless be expressed in xylem anatomical traits not captured by radial growth alone, underscoring the need for other proxies, such as quantitative wood anatomy, to fully assess disturbance impacts on climate sensitivity.

CRediT authorship contribution statement

Edurne Martinez del Castillo: Writing – review & editing. **Frederick Reinig:** Writing – review & editing. **Jan Esper:** Writing – review & editing, Funding acquisition. **Ingo Heinrich:** Writing – review & editing, Resources. **Emanuele Ziaco:** Writing – review & editing, Supervision, Funding acquisition, Conceptualization. **Antonia Kölzer:** Writing – original draft, Visualization, Methodology, Investigation, Formal analysis, Data curation, Conceptualization. **Davide Frigo:** Writing – review & editing, Visualization. **Gianluca Piovesan:** Writing – review & editing, Resources. **Burkhard Neuwirth:** Writing – review & editing, Resources. **Michele Baliva:** Writing – review & editing.

Funding

This work was supported by the German Science Foundation (524835176, ARiD–539441548; ES 161/15–1); the ERC Advanced Grant MONOSTAR (AdG 882727); the co-funded EU project AdAgriF (CZ.02.01.01/00/22_008/0004635), and the ERC Synergy project SYNERGY-PLAGUE (101118880).

Declaration of Competing Interest

The authors declare that they have no known competing financial interests or personal relationships that could have appeared to influence the work reported in this paper.

Acknowledgements

Special thanks to the staff of the Müritz National Park, Kellerwald-Edersee National Park, and Pollino National Park for logistic support. Comments from two anonymous reviewers greatly improved an original version of the manuscript.

Appendix A. Supporting information

Supplementary data associated with this article can be found in the online version at doi:10.1016/j.dendro.2026.126537.

Data availability

Data will be made available on request.

References

Abatzoglou, J.T., Dobrowski, S.Z., Parks, S.A., Hegewisch, K.C., 2018. TerraClimate, a high-resolution global dataset of monthly climate and climatic water balance from 1958 to 2015. Sci. Data 5, 170191. https://doi.org/10.1038/sdata.2017.191.

Abd Latif, Z., Blackburn, G.A., 2010. The effects of gap size on some microclimate variables during late summer and autumn in a temperate broadleaved deciduous forest. Int. J. Biometeorol. 54, 119–129. https://doi.org/10.1007/s00484-009-0260-1.

Adhikari, Y., Bachstein, N., Gohr, C., Blumröder, J.S., Meier, C., Ibisch, P.L., 2024. Old-growth beech forests in Germany as cool islands in a warming landscape. Sci. Rep. 14, 30311. https://doi.org/10.1038/s41598-024-81209-0.

Adhikari, Y., Blumröder, J.S., Meier, C., Ibisch, P.L., 2025. Beech buffers: Microclimate regulation in temperate old-growth forests, surroundings and forest edge. Ecol. Ind. 178, 114111. https://doi.org/10.1016/j.ecolind.2025.114111.

Altman, J., Fibich, P., Dolezal, J., Aakala, T., 2014. TRADER: a package for tree ring analysis of disturbance events in R. Dendrochronologia 32, 107–112. https://doi.org/10.1016/j.dendro.2014.01.004.

Altman, J., Fibich, P., Trotsiuk, V., Altmanova, N., 2024. Global pattern of forest disturbances and its shift under climate change. Sci. Total Environ. 915, 170117. https://doi.org/10.1016/j.scitotenv.2024.170117.

Babst, F., Bouriaud, O., Poulter, B., Trouet, V., Girardin, M.P., Frank, D.C., 2019. Twentieth century redistribution in climatic drivers of global tree growth. Sci. Adv. 5, eaat4313. https://doi.org/10.1126/sciadv.aat4313.

Baliva, M., Palli, J., Perri, F., Iovino, F., Luzzi, G., Piovesan, G., 2024. The return of tall forests: Reconstructing the canopy resilience of an extensively harvested primary forest in Mediterranean mountains. Sci. Total Environ. 953, 175806. https://doi.org/10.1016/j.scitotenv.2024.175806.

Black, B.A., Abrams, M.D., 2003. Use of boundary-line growth patterns as a basis for dendroecological release criteria. Ecol. Appl. 13, 1733–1749.

Black, B.A., Abrams, M.D., 2004. Development and application of boundary-line release criteria. Dendrochronologia 22, 31–42. https://doi.org/10.1016/j.dendro.2004.09.004.

Black, B.A., Abrams, M.D., Rentch, J.S., Gould, P.J., 2009. Properties of boundary-line release criteria in North American tree species. Ann. For. Sci. 66, 205–2015. https://doi.org/10.1051/forest/2008087.

Bontemps, J.-D., Esper, J., 2011. Statistical modelling and RCS detrending methods provide similar estimates of long-term trend in radial growth of common beech in north-eastern France. Dendrochronologia 29, 99–107. https://doi.org/10.1016/j.dendro.2010.09.002.

Bosela, M., Lukac, M., Castagneri, D., Sedmák, R., Biber, P., Carrer, M., Konôpka, B., Nola, P., Nagel, T.A., Popa, I., Roibu, C.C., Svoboda, M., Trotsiuk, V., Büntgen, U., 2018. Contrasting effects of environmental change on the radial growth of co-occurring beech and fir trees across Europe. Sci. Total Environ. 615, 1460–1469. https://doi.org/10.1016/j.scitotenv.2017.09.092.

Bunn, A.G., 2008. A dendrochronology program library in R (dplR). Dendrochronologia 26, 115–124. https://doi.org/10.1016/j.dendro.2008.01.002.

Cavin, L., Jump, A.S., 2017. Highest drought sensitivity and lowest resistance to growth suppression are found in the range core of the tree *Fagus sylvatica* L. not the equatorial range edge. Glob. Change Biol. 23, 362–379. https://doi.org/10.1111/gcb.13366.

Colangelo, M., Camarero, J.J., Gazol, A., Piovesan, G., Borghetti, M., Baliva, M., Gentilesca, T., Rita, A., Schettino, A., Ripullone, F., 2021. Mediterranean old-growth forests exhibit resistance to climate warming. Sci. Total Environ. 801, 149684. https://doi.org/10.1016/j.scitotenv.2021.149684.

Cook, E.R., Kairiukstis, L.A., 1990. Methods of Dendrochronology. Springer Netherlands, Dordrecht. https://doi.org/10.1007/978-94-015-7879-0.

Cornes, R.C., Van Der Schrier, G., Van Den Besselaar, E.J.M., Jones, P.D., 2018. An Ensemble Version of the E-OBS temperature and precipitation data sets. JGR Atmospheres 123, 9391–9409. https://doi.org/10.1029/2017JD028200.

van der Maaten, E., 2012. Climate sensitivity of radial growth in European beech (Fagus sylvatica L.) at different aspects in southwestern Germany. Trees 26, 777–788. https://doi.org/10.1007/s00468-011-0645-8.

Di Filippo, A., Biondi, F., Čufar, K., De Luis, M., Grabner, M., Maugeri, M., Presutti Saba, E., Schirone, B., Piovesan, G., 2007. Bioclimatology of beech (*Fagus sylvatica* L.) in the Eastern Alps: spatial and altitudinal climatic signals identified through a tree-ring network. J. Biogeogr. 34, 1873–1892. https://doi.org/10.1111/j.1365-2699.2007.01747.x.

Diers, M., Weigel, R., Leuschner, C., 2023. Both climate sensitivity and growth trend of European beech decrease in the North German Lowlands, while Scots pine still thrives, despite growing sensitivity. Trees 37, 523–543. https://doi.org/10.1007/s00468-022-02369-y.

Dorado-Liñán, I., Akhmetzyanov, L., Menzel, A., 2017. Climate threats on growth of rear-edge European beech peripheral populations in Spain. Int. J. Biometeorol. 61, 2097–2110. https://doi.org/10.1007/s00484-017-1410-5.

Druckenbrod, D.L., Cook, E.R., Pederson, N., Martin-Benito, D., 2024. Detrending tree-ring widths in closed-canopy forests for climate and disturbance history reconstructions. Dendrochronologia, 126195. https://doi.org/10.1016/j.dendro.2024.126195.

Duursma, R.A., 2015. Plantecophys - An R package for analysing and modelling leaf gas Exchange data. PLoS ONE 10, e0143346. https://doi.org/10.1371/journal.pone.0143346.

Esper, J., Torbenson, M., Büntgen, U., 2024. 2023 summer warmth unparalleled over the past 2,000 years. Nature 631, 94–97. https://doi.org/10.1038/s41586-024-07512-y.

Feoli, E., Lagonegro, M., 1982. Syntaxonomical analysis of beech woods in the Apennines (Italy) using the program package IAHOPA. Vegetatio 50, 129–173. https://doi.org/10.1007/BF00364109.

Frankovič, M., Janda, P., Mikoláš, M., Čada, V., Kozák, D., Pettit, J.L., Nagel, T.A., Buechling, A., Matula, R., Trotsiuk, V., Gloor, R., Dušátko, M., Kameniar, O., Vostarek, O., Lábusová, J., Ujházy, K., Synek, M., Begović, K., Ferenčík, M., Svoboda, M., 2021. Natural dynamics of temperate mountain beech-dominated primary forests in Central Europe. For. Ecol. Manag. 479, 118522. https://doi.org/10.1016/j.foreco.2020.118522.

Friedrichs, D.A., Trouet, V., Büntgen, U., Frank, D.C., Esper, J., Neuwirth, B., Löffler, J., 2009. Species-specific climate sensitivity of tree growth in Central-West Germany. Trees 23, 729–739. https://doi.org/10.1007/s00468-009-0315-2.

Gray, A.N., Spies, T.A., Pabst, R.J., 2012. Canopy gaps affect long-term patterns of tree growth and mortality in mature and old-growth forests in the Pacific Northwest. For. Ecol. Mana. 281, 111–120. https://doi.org/10.1016/j.foreco.2012.06.035.

Guiot, J., 1991. The bootstrapped response function. Tree-Ring Bull. 51, 39–41.

Hacket-Pain, A., Szymkowiak, J., Journé, V., Barczyk, M.K., Thomas, P.A., Lageard, J.G. A., Kelly, D., Bogdziewicz, M., 2025. Growth decline in European beech associated with temperature-driven increase in reproductive allocation. Proc. Natl. Acad. Sci. U. S. A. 122, e2423181122. https://doi.org/10.1073/pnas.2423181122.

Hacket-Pain, A.J., Ascoli, D., Vacchiano, G., Biondi, F., Cavin, L., Conedera, M., Drobyshev, I., Liñán, I.D., Friend, A.D., Grabner, M., Hartl, C., Kreyling, J., Lebourgeois, F., Levanič, T., Menzel, A., Van Der Maaten, E., Van Der Maaten-Theunissen, M., Muffler, L., Motta, R., Roibu, C., Popa, I., Scharnweber, T., Weigel, R., Wilmking, M., Zang, C.S., 2018. Climatically controlled reproduction drives interannual growth variability in a temperate tree species. Ecol. Lett. 21, 1833–1844. https://doi.org/10.1111/ele.13158.

Harris, I., Osborn, T.J., Jones, P., Lister, D., 2020. Version 4 of the CRU TS monthly high-resolution gridded multivariate climate dataset. Sci. Data 7, 109. https://doi.org/10.1038/s41597-020-0453-3.

Harvey, J.E., Smiljanić, M., Scharnweber, T., Buras, A., Cedro, A., Cruz-García, R., Drobyshev, I., Janecka, K., Jansons, Ā., Kaczka, R., Klisz, M., Läänelaid, A., Matisons, R., Muffler, L., Sohar, K., Spyt, B., Stolz, J., Van Der Maaten, E., Van Der Maaten-Theunissen, M., Vitas, A., Weigel, R., Kreyling, J., Wilmking, M., 2020. Tree growth influenced by warming winter climate and summer moisture availability in northern temperate forests. Glob. Change Biol. 26, 2505–2518. https://doi.org/10.1111/gcb.14966.

Holmes, R.L., 1983. Computer assisted quality control in tree-ring dating and measurement. Tree-Ring Bull. 43, 69–78.

Hughes, M.K., Swetnam, T.W., Diaz, H.F., 2011. Dendroclimatology: Progress and Prospects. Developments in Paleoenvironmental Research. Springer Netherlands, Dordrecht. https://doi.org/10.1007/978-1-4020-5725-0.

Hughes, N.M., Sanchez, A., Berry, Z.C., Smith, W.K., 2024. Clouds and plant ecophysiology: missing links for understanding climate change impacts. Front. For. Glob. Change 7, 1330561. https://doi.org/10.3389/ffgc.2024.1330561.

Ionita, M., Nagavciuc, V., 2021. Changes in drought features at the European level over the last 120 years. Nat. Hazards Earth Syst. Sci. 21, 1685–1701. https://doi.org/10.5194/nhess-21-1685-2021.

Johnstone, J.F., Allen, C.D., Franklin, J.F., Frelich, L.E., Harvey, B.J., Higuera, P.E., Mack, M.C., Meentemeyer, R.K., Metz, M.R., Perry, G.L., Schoennagel, T., Turner, M. G., 2016. Changing disturbance regimes, ecological memory, and forest resilience. Front. Ecol. Environ. 14, 369–378. https://doi.org/10.1002/fee.1311.

Journé, V., Szymkowiak, J., Foest, J., Hacket-Pain, A., Kelly, D., Bogdziewicz, M., 2024. Summer solstice orchestrates the subcontinental-scale synchrony of mast seeding. Nat. Plants 10, 367–373. https://doi.org/10.1038/s41477-024-01651-w.

Jucker, T., 2022. Deciphering the fingerprint of disturbance on the three-dimensional structure of the world's forests. N. Phytol. 233, 612–617. https://doi.org/10.1111/nph.17729.

Kaiser, K., Kobel, Joachim, Küster, Mathias, Schwabe, Matthias, 2015. Neue beiträge zum naturraum und zur landschaftsgeschichte im teilgebiet serrahn des müritz-nationalparks. Geozon Sci. Media.

Kirchmeir, H., Kovarovics, A., 2020. Nomination Dossier 'Ancient and Primeval Beech Forests of the Carpathians and Other Regions of Europe' as extension to the existing Natural World Heritage Site (1133ter). Klagenfurt.

Lauer, W., Frankenberg, P., 1988. Klimaklassifikation der Erde. Geogr. Rundsch. 40, 55–59.

Lebourgeois, F., Bréda, N., Ulrich, E., Granier, A., 2005. Climate-tree-growth relationships of European beech (Fagus sylvatica L.) in the French Permanent Plot Network (RENECOFOR). Trees 19, 385–401. https://doi.org/10.1007/s00468-004-0397-9.

Leuschner, C., 2020. Drought response of European beech (Fagus sylvatica L.)—A review. Perspect. Plant Ecol. 47, 125576. https://doi.org/10.1016/j.ppees.2020.125576.

Li, T., He, B., Chen, D., Chen, H.W., Guo, L., Yuan, W., Fang, K., Shi, F., Liu, L., Zheng, H., Huang, L., Wu, X., Hao, X., Zhao, X., Jiang, W., 2024. Increasing sensitivity of tree radial growth to precipitation. Geophys. Res. Lett. 51, e2024GL110003. https://doi.org/10.1029/2024GL110003.

Martinez del Castillo, E., Torbenson, M.C.A., Reinig, F., Konter, O., Ziaco, E., Büntgen, U., Esper, J., 2024. Diverging growth trends and climate sensitivities of individual pine trees after the 1976 extreme drought. Sci. Total Environ. 946, 174370. https://doi.org/10.1016/j.scitotenv.2024.174370.

Martinez del Castillo, E., Zang, C.S., Buras, A., Hacket-Pain, A., Esper, J., Serrano-Notivoli, R., Hartl, C., Weigel, R., Klesse, S., Resco De Dios, V., Scharnweber, T., Dorado-Liñán, I., Van Der Maaten-Theunissen, M., Van Der Maaten, E., Jump, A., Mikac, S., Banzragch, B.-E., Beck, W., Cavin, L., Claessens, H., Čada, V., Čufar, K., Dulamsuren, C., Gričar, J., Gil-Pelegrín, E., Janda, P., Kazimirovic, M., Kreyling, J., Latte, N., Leuschner, C., Longares, L.A., Menzel, A., Merela, M., Motta, R., Muffler, L., Nola, P., Petritan, A.M., Petritan, I.C., Prislan, P., Rubio-Cuadrado, Á., Rydval, M., Stajić, B., Svoboda, M., Toromani, E., Trotsiuk, V., Wilmking, M., Zlatanov, T., De Luis, M., 2022. Climate-change-driven growth decline of European beech forests. Commun. Biol. 5, 163. https://doi.org/10.1038/s42003-022-03107-3.

Mausolf, K., Wilm, P., Härdtle, W., Jansen, K., Schuldt, B., Sturm, K., Von Oheimb, G., Hertel, D., Leuschner, C., Fichtner, A., 2018. Higher drought sensitivity of radial growth of European beech in managed than in unmanaged forests. Sci. Total Envir 642, 1201–1208. https://doi.org/10.1016/j.scitotenv.2018.06.065.

Müller-Haubold, H., Hertel, D., Seidel, D., Knutzen, F., Leuschner, C., 2013. Climate responses of aboveground productivity and allocation in fagus sylvatica: a transect study in mature forests. Ecosystems 16, 1498–1516. https://doi.org/10.1007/s10021-013-9698-4.

Muscolo, A., Bagnato, S., Sidari, M., Mercurio, R., 2014. A review of the roles of forest canopy gaps. J. For. Res. 25, 725–736. https://doi.org/10.1007/s11676-014-0521-7.

Nagel, T.A., Levanic, T., Diaci, J., 2007. A dendroecological reconstruction of disturbance in an old-growth Fagus-Abies forest in Slovenia. Ann. For. Sci. 64, 891–897. https://doi.org/10.1051/forest:2007067.

Nagel, T.A., Svoboda, M., Kobal, M., 2014. Disturbance, life history traits, and dynamics in an old-growth forest landscape of southeastern Europe. Ecol. Appl. 24, 663–679. https://doi.org/10.1890/13-0632.1.

Nowacki, G.J., Abrams, M.D., 1997. Radial-growth averaging criteria for reconstruction disturbance histories from presettlement-origin oaks. Ecol. Monogr. 67, 225. https://doi.org/10.2307/2963514.

Ols, C., Klesse, S., Girardin, M.P., Evans, M.E.K., DeRose, R.J., Trouet, V., 2023. Detrending climate data prior to climate–growth analyses in dendroecology: a common best practice? Dendrochronologia 79, 126094. https://doi.org/10.1016/j.dendro.2023.126094.

Pettit, J.L., Pettit, J.M., Janda, P., Rydval, M., Čada, V., Schurman, J.S., Nagel, T.A., Bače, R., Saulnier, M., Hofmeister, J., Matula, R., Kozák, D., Frankovič, M., Turcu, D. O., Mikoláš, M., Svoboda, M., 2021. Both cyclone-induced and convective storms drive disturbance patterns in european primary beech forests. JGR Atmospheres 126, e2020JD033929. https://doi.org/10.1029/2020JD033929.

Piovesan, G., Adams, J.M., 2001. Masting behaviour in beech: linking reproduction and climatic variation. Can. J. Bot. 79, 1039–1047. https://doi.org/10.1139/cjb-79-9-1039.

Piovesan, G., Di Filippo, A., Alessandrini, A., Biondi, F., Schirone, B., 2005b. Structure, dynamics and dendroecology of an old-growth *Fagus* forest in the Apennines. J. Veg. Sci. 16, 13–28. https://doi.org/10.1111/j.1654-1103.2005.tb02334.x.

Piovesan, G., Biondi, F., Bernabei, M., Di Filippo, A., Schirone, B., 2005a. Spatial and altitudinal bioclimatic zones of the Italian peninsula identified from a beech (Fagus sylvatica L.) tree-ring network. Acta Oecologica 27, 197–210. https://doi.org/10.1016/j.actao.2005.01.001.

Piovesan, G., Biondi, F., Baliva, M., De Vivo, G., Marchianò, V., Schettino, A., Di Filippo, A., 2019. Lessons from the wild: slow but increasing long-term growth allows for maximum longevity in European beech. Ecology 100, e02737. https://doi.org/10.1002/ecy.2737.

R Core Team, 2024. R: A Language and Environment for Statistical Computing. R Foundation for Statistical Computing, Vienna, Austria. https://www.R-project.org/.

Reddy, S.C., Arteman, M.L., Forrester, J.A., Keyser, T.L., 2025. Canopy gaps increase species-dependent edge tree diameter growth in a mature southern Appalachian mixed hardwood forest. For. Ecol. Manag. 595, 123008. https://doi.org/10.1016/j.foreco.2025.123008.

Reid, P.C., Hari, R.E., Beaugrand, G., Livingstone, D.M., Marty, C., Straile, D., Barichivich, J., Goberville, E., Adrian, R., Aono, Y., Brown, R., Foster, J., Groisman, P., Hélaouët, P., Hsu, H., Kirby, R., Knight, J., Kraberg, A., Li, J., Lo, T., Myneni, R.B., North, R.P., Pounds, J.A., Sparks, T., Stübi, R., Tian, Y., Wiltshire, K. H., Xiao, D., Zhu, Z., 2016. Global impacts of the 1980s regime shift. Glob. Change Biol. 22, 682–703. https://doi.org/10.1111/gcb.13106.

Roibu, C.-C., Palaghianu, C., Nagavciuc, V., Ionita, M., Sfecla, V., Mursa, A., Crivellaro, A., Stirbu, M.-I., Cotos, M.-G., Popa, A., Sfecla, I., Popa, I., 2022. The response of beech (Fagus sylvatica L.) populations to climate in the easternmost sites of its european distribution. Plants 11, 3310. https://doi.org/10.3390/plants11233310.

Rubino, D.L., McCarthy, B.C., 2004. Comparative analysis of dendroecological methods used to assess disturbance events. Dendrochronologia 21, 97–115. https://doi.org/10.1078/1125.7865.00047.

Rydval, M., Druckenbrod, D.L., Svoboda, M., Trotsiuk, V., Janda, P., Mikoláš, M., Čada, V., Bače, R., Teodosiu, M., Wilson, R., 2018. Influence of sampling and disturbance history on climatic sensitivity of temperature-limited conifers. Holocene 28, 1574–1587. https://doi.org/10.1177/0959683618782605.

Seidl, R., Thom, D., Kautz, M., Martin-Benito, D., Peltoniemi, M., Vacchiano, G., Wild, J., Ascoli, D., Petr, M., Honkaniemi, J., Lexer, M.J., Trotsiuk, V., Mairota, P., Svoboda, M., Fabrika, M., Nagel, T.A., Reyer, C.P.O., 2017. Forest disturbances under climate change. Nat. Clim. Change 7, 395–402. https://doi.org/10.1038/nclimate3303.

Seidl, R., Potterf, M., Müller, J., Turner, M.G., Rammer, W., 2024. Patterns of early post-disturbance reorganization in Central European forests. Proc. R. Soc. B. 291, 20240625. https://doi.org/10.1098/rspb.2024.0625.

Selås, V., Piovesan, G., Adams, J.M., Bernabei, M., 2002. Climatic factors controlling reproduction and growth of Norway spruce in southern Norway. Can. J. For. Res. 32, 217–225. https://doi.org/10.1139/x01-192.

Serrano-Notivoli, R., Jevšenak, J., Martinez Del Castillo, E., Čufar, K., Škrk-Dolar, N., Battipaglia, G., Camarero, J.J., Pain, A.H., Jump, A., Motta, R., Nola, P., Panayotov, M., Petritan, I.C., Popa, A., Popa, I., Roibu, C.-C., Svoboda, M., Zang, C., Zlatanov, T., Balzano, A., Biondi, F., Čada, V., Dimitrov, D.P., Gričar, J., Janda, P., Keren, S., Lebourgeois, F., Li, G., Longares, L.A., Lukić, I., Merela, M., Mikac, S., Novak, K., Petritan, A.M., Prislan, P., Roibu, A.-M., Rubio-Cuadrado, A., Rydval, M., Saz, M.Á., Tejedor, E., Tegel, W., Tognetti, R., Toromani, E., Trotsiuk, V., Turcu, D., De Luis, M., 2025. A single-tree approach to determine climate-growth patterns of European beech and their seasonality in the species southern distribution area. Agr. For. Meteor. 371, 110644. https://doi.org/10.1016/j.agrformet.2025.110644.

Spinoni, J., Naumann, G., Vogt, J., Barbosa, P., 2015. European drought climatologies and trends based on a multi-indicator approach. Glob. Plan. Change 127, 50–57. https://doi.org/10.1016/j.gloplacha.2015.01.012.

Splechtna, B.E., Gratzer, G., Black, B.A., 2005. Disturbance history of a European old-growth mixed-species forest—A spatial dendro-ecological analysis. J. Veg. Sci. 16, 511–522. https://doi.org/10.1111/j.1654-1103.2005.tb02391.x.

Tong, R., Ji, B., Wang, G.G., Lou, C., Ma, C., Zhu, N., Yuan, W., Wu, T., 2024. Canopy gap impacts on soil organic carbon and nutrient dynamic: a meta-analysis. Ann. For. Sci. 81, 12. https://doi.org/10.1186/s13595-024-01224-z.

Toreti, A., Belward, A., Perez-Dominguez, I., Naumann, G., Luterbacher, J., Cronie, O., Seguini, L., Manfron, G., Lopez-Lozano, R., Baruth, B., Van Den Berg, M., Dentener, F., Ceglar, A., Chatzopoulos, T., Zampieri, M., 2019. The exceptional 2018 European water seesaw calls for action on adaptation. Earth'S. Future 7, 652–663. https://doi.org/10.1029/2019EF001170.

Trotsiuk, V., Hobi, M.L., Commarmot, B., 2012. Age structure and disturbance dynamics of the relic virgin beech forest Uholka (Ukrainian Carpathians). For. Ecol. Manag 265, 181–190. https://doi.org/10.1016/j.foreco.2011.10.042.

Turner, M.G., 2010. Disturbance and landscape dynamics in a changing world. Ecology 91, 2833–2849. https://doi.org/10.1890/10-0097.1.

Vacchiano, G., Garbarino, M., Lingua, E., Motta, R., 2017. Forest dynamics and disturbance regimes in the Italian Apennines. For. Ecol. Manag 388, 57–66. https://doi.org/10.1016/j.foreco.2016.10.033.

Veblen, T.T., Hadley, K.S., Reid, M.S., 1991. Disturbance and stand development of a colorado subalpine forest. J. Biogeogr. 18, 707. https://doi.org/10.2307/2845552.

Vicente-Serrano, S.M., Beguería, S., López-Moreno, J.I., 2010. A multiscalar drought index sensitive to global warming: the standardized precipitation evapotranspiration index. J. Clim. 23, 1696–1718. https://doi.org/10.1175/2009JCLI2909.1.

Vitasse, Y., Bottero, A., Cailleret, M., et al., 2019. Contrasting resistance and resilience to extreme drought and late spring frost in five major European tree species. Glob. Chang. Biol. 25, 3781–3792. https://doi.org/10.1111/gcb.14803.

von Oheimb, G., Westphal, C., Tempel, H., Härdtle, W., 2005. Structural pattern of a near-natural beech forest (Fagus sylvatica) (Serrahn, North-east Germany). For. Ecol. Manag 212, 253–263. https://doi.org/10.1016/j.foreco.2005.03.033.

Wigley, T.M.L., Briffa, K.R., Jones, P.D., 1984. On the average value of correlated time series, with applications in dendroclimatology and hydrometeorology. J. Clim. Appl. Meteor 23, 201–213. https://doi.org/10.1175/15200450(1984)023<0201:OTAVOC>2.0.CO;2.

Wild, M., 2009. Global dimming and brightening: a review. J. Geophys. Res. 114, 2008JD011470. https://doi.org/10.1029/2008JD011470.

Wild, M., Gilgen, H., Roesch, A., Ohmura, A., Long, C.N., Dutton, E.G., Forgan, B., Kallis, A., Russak, V., Tsvetkov, A., 2005. From dimming to brightening: decadal changes in Solar Radiation at Earth's Surface. Science 308, 847–850. https://doi.org/10.1126/science.1103215.

Ziaco, E., Di Filippo, A., Alessandrini, A., Baliva, M., D'andrea, E., Piovesan, G., 2012. Old-growth attributes in a network of Apennines (Italy) beech forests: disentangling the role of past human interferences and biogeoclimate. Plant Biosyst. 146, 153–166. https://doi.org/10.1080/11263504.2011.650729.

Zohner, C.M., Mo, L., Renner, S.S., Svenning, J.-C., Vitasse, Y., Benito, B.M., Ordonez, A., Baumgarten, F., Bastin, J.-F., Sebald, V., Reich, P.B., Liang, J., Nabuurs, G.-J., de-Miguel, S., Alberti, G., Antón-Fernández, C., Balazy, R., Brändli, U.-B., Chen, H.Y.H., Chisholm, C., Cienciala, E., Dayanandan, S., Fayle, T.M., Frizzera, L., Gianelle, D., Jagodzinski, A.M., Jaroszewicz, B., Jucker, T., Kepfer-Rojas, S., Khan, M.L., Kim, H. S., Korjus, H., Johannsen, V.K., Laarmann, D., Lang, M., Zawila-Niedzwiecki, T., Niklaus, P.A., Paquette, A., Pretzsch, H., Saikia, P., Schall, P., Šebeň, V., Svoboda, M., Tikhonova, E., Viana, H., Zhang, C., Zhao, X., Crowther, T.W., 2020. Late-spring frost risk between 1959 and 2017 decreased in North America but increased in Europe and Asia. Proc. Natl. Acad. Sci. U. S. A. 117, 12192–12200. https://doi.org/10.1073/pnas.1920816117.